A fluid model for ion heating due to ionization in a plasma flow

M. A. Dorf,[a)] V. E. Semenov, and V. G. Zorin
Institute of Applied Physics, Russian Academy of Sciences, 603600, Nizhny Novgorod, Russia

(Received 26 February 2008; accepted 6 August 2008; published online 5 September 2008)

A mechanism of ion heating due to local ionization in a plasma flow with hot electrons and initially cold ions is described. It is shown that the ion temperature can increase significantly as the ions are accelerated to the ion-acoustic speed, provided there is significant ionization in the acceleration region. The fluid model describing ionization ion heating includes particle, momentum, and energy balance equations for ion species. Using this model with parameters characteristic of gas-dynamic electron cyclotron resonance (ECR) ion source SMIS 37 yields much higher effective ion temperature than can be attributed to the electron-ion collisional energy transfer, typically considered for classical ECR ion sources. This theoretical result is found to be in agreement with findings of recent experiments carried out in SMIS 37. © *2008 American Institute of Physics*.
[DOI: 10.1063/1.2976367]

I. INTRODUCTION

Even for a simple case of a plasma contained in the chamber, the electric field in the quasi-neutral plasma bulk (presheath) will accelerate ions to the chamber walls such that the ion current balances the electron current to the walls. This fundamental problem of the ion flow in the plasma presheath has been extensively studied by means of fluid equations and using a kinetic approach for various collisionality regimes and methods of ion generation.[1–7] Details of the ion distribution function in the plasma presheath were first studied by Tonks and Langmuir in 1929, when they were investigating the problem of a glow discharge.[1] Ions born from ionization of background gas in the plasma presheath are accelerated by the electric field toward the wall. Tonks and Langmuir considered collisionless regime of ion acceleration, therefore cold ions originated at different positions arrive to the wall with different velocities, providing velocity spread that one can interpret as the effective ion temperature. A similar mechanism of ion heating can be provided by means of charge-exchange collisions in the plasma presheath, and was studied by Riemann.[5] A collisional model of the plasma preasheath taking into account ion-neutral and ion-ion collisions, as well as background gas ionization was presented by Scheuer and Emmert.[6,7] Evolution of the ion distribution function as the ions are accelerated to the wall was studied. However, the ion temperature in the bulk of the plasma was assumed to be on the order of the electron temperature, hence no essential dynamic of the ion temperature (in particular, strong ion heating) was obtained. In our modeling, similarly to Scheuer and Emmert, we consider both ionization and strong ion-ion collisions, but with initially cold ions; and therefore can obtain significant ion heating as the ions are accelerated to the ion-acoustic speed.

The recent advances in the ECR ion plasma source technology[8] motivate studies of the ion temperature evolution in the plasma presheath. Indeed, the extracted ion beam temperature is one of the most important parameters of an ion source; hence, high emphasis is placed on studies of the mechanisms of ion heating. In a typical ECR ion source electrons are quickly heated by the microwave radiation, the ions born from ionization of a background gas are cold, and ion-ion collisions are dominant. Therefore, in the present work we describe ion heating provided by ionization in a plasma flow with hot electrons and initially cold ions. We consider strong ion-ion collisionality regime of ion acceleration typical for ECR ion sources, where the mean free path for ion-ion collisions (λ_{ii}) is much less than a characteristic length of the electrostatic potential variation. A set of fluid equations is used to describe the evolution of the ion density n, velocity V, and temperature T_i, in the presence of neutral gas ionization and an ambipolar plasma potential. It is shown that the temperature of initially cold ($T_i \ll T_e$) and slow ($V_i \ll V_s$) ions can be significantly increased as the ion flow is accelerated to the ion-acoustic speed, i.e., $V_s = \sqrt{(Z_i T_e + \gamma T_i)/m_i}$, where T_e is the electron temperature and Z_i, m_i, and γ are the ion charge state, mass, and the adiabatic gamma-factor, respectively. This acceleration is typical for plasma ion sources where the ion flow has to reach the ion-acoustic speed inside the plasma bulk to break the quasi-neutrality condition in the vicinity of an extraction electrode.

The proposed hydrodynamic model is applied to describe ion heating in a magnetic trap with the quasi-gas-dynamic regime of plasma confinement. The quasi-gas-dynamic regime of confinement[9–17] is characterized by short ion mean free path ($\lambda_{ii} \ll L$) and high electron-ion collision frequency ($\nu_{ei} \gg V_s/L$). Here, L is the characteristic length of the magnetic trap. Plasma lifetime τ is determined by gas-dynamic ion escape from the trap with the ion-acoustic speed, i.e., $\tau = L/V_s$, and the loss cone is filled with electrons, provided by $\nu_{ei} \gg 1/\tau$. Electron mean free path is comparable to the trap length, and the fluid equations are only applied to the ion flow, which is accelerated from almost zero velocity in the center of the trap to the ion-acoustic speed in the magnetic plug. Note that the quasi-gas-dynamic regime of plasma confinement provides more intense ion flows from the magnetic plug with lower ion charge states compared to

[a)]Present address: Plasma Physics Laboratory, Princeton, NJ 08543, USA.

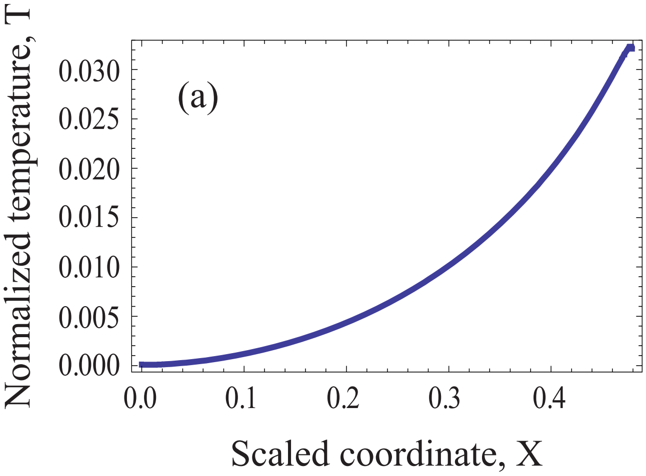

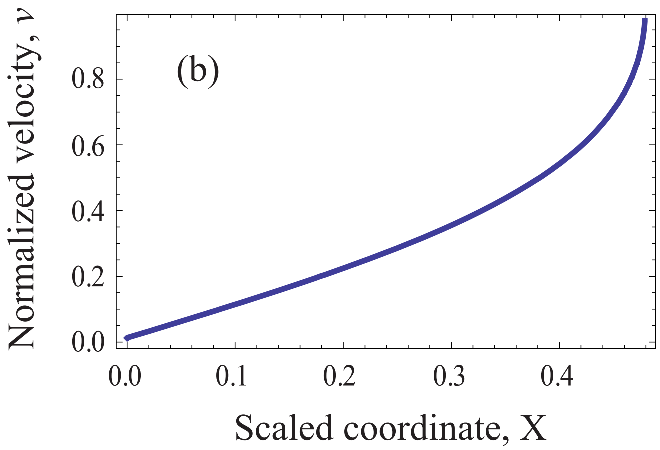

FIG. 1. (Color online) Spatial evolution of the ion flow parameters: (a) Normalized ion flow temperature T; (b) normalized flow velocity υ. $T(0)=10^{-4}$, $\upsilon(0)=\sqrt{\gamma T(0)}$, $\gamma=5/3$. Constant flow cross-section area is assumed.

the classical regime of confinement with the empty electron loss cone. Recently, the concept of quasi-gas-dynamic confinement was successfully utilized in a gas-dynamic ECR source of multicharged ions SMIS 37.[12–17] The latest experiments on the SMIS 37 stand demonstrated rather high values of the extracted ion beam temperature[17] that cannot be explained by means of the collisional heating mechanisms that is the collisional energy transfer from hot electrons to cold ions. In this paper, we demonstrate that ion heating due to ionization in a plasma flow can result in the ion temperature comparable to that measured in the SMIS 37 experiments.

II. THEORETICAL MODEL

In this section we consider a set of one-dimensional fluid equations governing spatial evolution of the stationary ion flow in plasma. Taking into account ionization of the background gas by electrons, the continuity equation is given by

$$d(SVn)/dx = J. \tag{1}$$

Here, x is the coordinate along the flow propagation, S, V, and n are the cross-section area, velocity, and number density of the ion flow, respectively, and $J=Z_i n n_a S K_i$, where n_a is the number density of neutral atoms and K_i is the ionization rate. Assuming quasi-neutrality, i.e., $n_e \approx Z_i n$, and Boltzmann distribution of electrons, the electrostatic ambipolar field in a plasma is given by $E_s=-(T_e/en)dn/dx$, where e is the electron charge; and we readily obtain the following equation governing the evolution of the ion flow momentum:

$$\frac{d}{dx}(nV^2S) + S\frac{d}{dx}\left(n\frac{T_i}{m_i}\right) = -S\frac{Z_iT_e}{m_i}\frac{dn}{dx}. \tag{2}$$

The energy conservation equation takes the following form:

$$\frac{d}{dx}\left(\frac{nV^3S}{2} + \frac{\gamma}{\gamma-1}\frac{T_i}{m_i}nVS\right) = -SV\frac{Z_iT_e}{m_i}\frac{dn}{dx}. \tag{3}$$

In Eqs. (2) and (3) it is assumed that neutral atoms have negligible temperature and directed velocity. The boundary conditions for the set of equations (1)–(3) are $n(0)=n_0$, $T_i(0)=T_{i0}$, and $V(0)=V_0$. We now solve Eqs. (1)–(3) for dV/dx and dT_i/dx variables, and readily obtain

$$dT_i/dx = A_TJ + B_TdS/dx, \tag{4}$$

$$dV/dx = A_VJ + B_VdS/dx, \tag{5}$$

where the matrix coefficients A_T, A_V, B_T, B_V are given by

$$A_T = \frac{\left[V^4(1-\gamma) + V^2\left(\frac{3T_i + Z_iT_e\gamma}{m_i} - V_s^2\right) - 2\gamma\frac{T_i^2 + Z_iT_eT_i}{m_i^2}\right]}{2nVS(V_s^2 - V^2)/m_i}, \tag{6}$$

$$B_T = [V^2T_i(\gamma-1)]/[S(V_s^2 - V^2)], \tag{7}$$

$$A_V = [V^2(\gamma+1) + 2Z_iT_e/m_i]/[2nS(V_s^2 - V^2)], \tag{8}$$

$$B_V = -[V(\gamma T_i + Z_iT_e)]/[m_iS(V_s^2 - V^2)]. \tag{9}$$

Note that for the case of the initially cold and slow ion flow, $B_T<0$ and $B_V>0$; therefore, a decrease in the flow cross-section area provides an increase in the flow velocity and decrease in the ion temperature. However, the ion temperature can be increased by means of ionization. For simplicity, we now consider constant flow cross-section area: $dS/dx=0$. Equations (4)–(6) and (8) show that for $V_0 \ll V_s$, the temperature decreases ($A_T<0$), and the flow velocity increases ($A_V>0$). However, as the ion flow velocity reaches the critical value V_{cr} corresponding to the zero of A_T, the ion temperature starts to grow. Note that for the case of $V_0 \ll V_s$ and $T_i \ll T_e$,

$$V_{cr}^2 \cong \frac{2\gamma}{\gamma-1}\frac{T_i}{m_i}, \tag{10}$$

which is the order of the ion thermal velocity.

Illustrative numerical solution to Eqs. (1)–(3) for the case of the constant flow cross-section area $S(x)=S_0$ is plotted in Fig. 1. Note that the following normalized ion flow parameters are introduced to provide a convenient graphical representation of the results: the normalized temperature $T=T_i/Z_iT_e$, the normalized flow velocity $\nu=V/\sqrt{Z_iT_e/m_i}$ and the scaled coordinate $X=\int_0^x J(x')dx'/(n_0 S_0\sqrt{Z_i T_e/m_i})$. Figure 1(a) shows that the ion temperature increases significantly as the flow velocity approaches the ion-acoustic speed. Note that for the case of a constant cross-section area, the laminar flow solution can not be continued behind the singularity point corresponding to $V=V_s$. However, the flow transition into the supersonic regime can be provided by means of the flow area variations.

Numerical studies of Eqs. (1)–(3) for the case of a constant cross-section area demonstrate a week dependency of the final ion flow temperature (when $V=V_s$) on the initial conditions V_0, T_{i0} provided that they are sufficiently small, namely, $V_0 \ll V_s$, $T_{i0} \ll T_e$. Moreover, the final value of the flow temperature can be estimated analytically for the case of $V_0 \ll V_s$, $T_{i0} \ll T_e$, and $S=\text{const}$. Integration of Eq. (2) readily gives $n(m_i V^2+T_i)\approx Z_i T_e(n_0-n)$. Figure 1 shows that T_i is much less than $Z_i T_e$; hence, $n\approx n_0 Z_i T_e/(m_i V^2+Z_i T_e)$, and integration of Eq. (3) readily gives the following value of the final ion flow temperature:

$$T_f \approx 0.07\frac{\gamma-1}{\gamma}Z_i T_e, \tag{11}$$

which is consistent with the numerical solution illustrated in Fig. 1(b).

It should be noted that the ion flux, i.e., $\Gamma=nVS$, leaving the acceleration region is much larger than the initial ion flux at $x=0$. Indeed, the ratio of the final to initial ion flow velocity is much greater than unity, i.e., $V_s/V_0 \gg 1$, whereas the ion density decreases only by the factor of $(m_i V_s^2+Z_i T_e)/(m_i V_0^2+Z_i T_e)\approx 2$. Therefore, most of the plasma is created in the acceleration region provided by a significant ionization.

III. ION HEATING IN A GAS-DYNAMIC ECR SOURCE OF MULTICHARGED IONS

In this section, we use the above theoretical model with parameters typical for the SIMS 37 gas-dynamic ECR ion source to estimate the effective ion temperature due to ionization heating. ECR gas breakdown is produced by high-power ($\approx$100 kW) pulsed ($\approx$1.5 ms) microwave (37 GHz) radiation, and the device utilizes a concept of the quasi-gas-dynamic regime of plasma confinement in a magnetic trap. This regime of plasma confinement in a magnetic trap is characterized by strong electron-ion collisions; i.e., $\nu_{ei} \gg V_s/L$. Plasma lifetime is determined by gas-dynamic ion escape from the trap with the ion-sound speed, i.e., $\tau=L/V_s$, and the loss cone is filled with electrons, provided by $\nu_{ei} \gg 1/\tau$. The electron mean free path is comparable to the trap length, and the electrons are confined by variations in electrostatic potential between the center of the magnetic trap and the extraction electrode (one of the chamber walls). Note that the electrons suffer enough collisions during the plasma lifetime and are distributed according to the Boltzmann distribution law. The schematic of the ion source is shown in Fig. 2(a), and detailed information regarding the SMIS 37 device parameters and principles of operation can be found in Refs. 12–17. The ion flow, bounded by the magnetic flux tube, is leaving the plug toward the extraction electrode. Recent experiments with nitrogen demonstrated that the current density of the ion flow leaving the magnetic plug can reach ~1 A/cm^2, with the single and double ionized ions present in the flow at almost the same level. However, if the mean free path for ion-ion collisions (λ_{ii}) is much less than the characteristic length L of the trap, then all ion species can be considered as a single fluid with a charge state averaged over all ion species.

Regardless the regime of plasma confinement (classical or quasi-gas-dynamic), the effective ion temperature attributed to the collisional energy transfer from the hot electrons to the cold ions can be estimated from the following relation:[18]

$$n_e(T_e-T_i)\nu_{ei}^E \sim n_i T_i/\tau. \tag{12}$$

Here, n_e and n_i are the electron and ion densities, respectively, τ is the plasma lifetime in the trap, and ν_{ie}^E is the electron-ion energy equipartition rate given by[19]

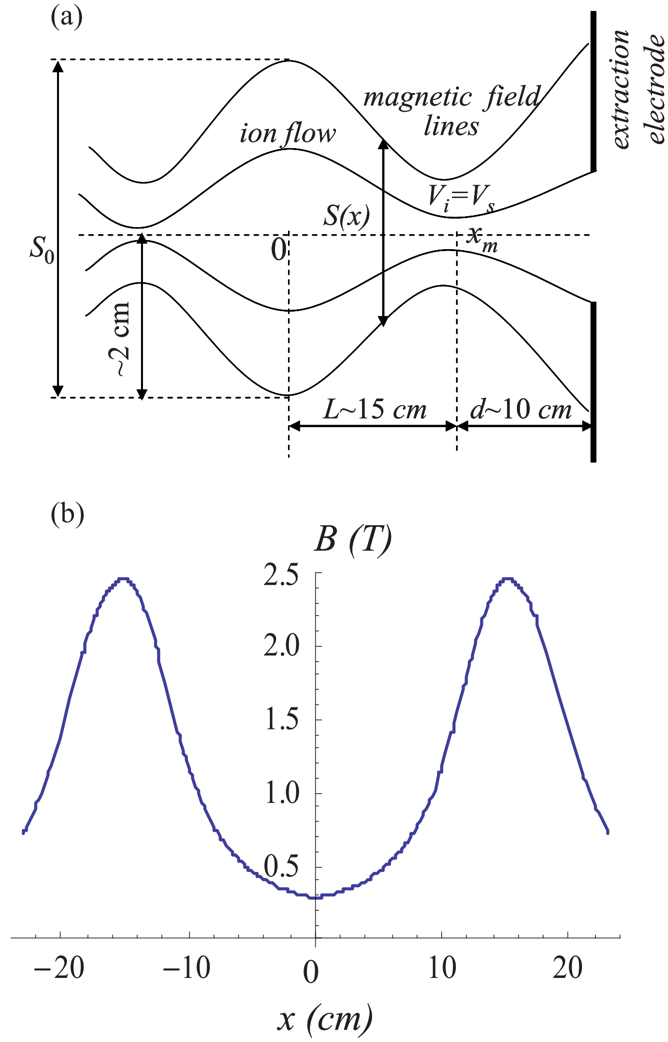

FIG. 2. (Color online) (a) Schematic of the ion flow in the magnetic trap of the SMIS 37 device; (b) the on-axis magnetic field profile $B(x)$.

$$\nu_{ie}^{E}\,[\mathrm{s}^{-1}] = \frac{3.2\times 10^{-9}\ln\Lambda_{ei}}{T_e^{3/2}\,[\mathrm{eV}]}\frac{n_i\,[\mathrm{cm}^{-3}]Z_i^2}{A_i}, \quad (13)$$

where A_i is the ion atomic mass number, and Λ_{ei} is the Coulomb logarithm. Plasma lifetime τ for the gas-dynamic ion source is determined by

$$\tau \sim L/V_s \cong L/\sqrt{\langle Z\rangle T_e/m_i}, \quad (14)$$

where $\langle Z\rangle$ is the charge state averaged over all species. For a typical regime of ion extraction in SMIS 37 $T_e \sim 70$ eV, $n_e \approx \langle Z\rangle \cdot n_i$, $n_i \sim 10^{13}$ cm^{-3}, $\langle Z\rangle \sim 1.5$, $L=15$ cm, $A_i=14$, and one can readily obtain the following value for the ion temperature: $T_i \sim 0.05$ eV. Note that the ion mean free path corresponding to this value of ion temperature is much less than the trap length $\lambda_{ii} \ll L$. Here, $\lambda_{ii} \approx V_s/\nu_{ii}$, and the ion-ion collision frequency ν_{ii} is given by $\nu_{ii}\,[\mathrm{s}^{-1}]=6.8\times 10^{-8}\ln\Lambda_{ii}/T_i^{3/2}\,[\mathrm{eV}]Z_i^4 n_i\,[\mathrm{cm}^{-3}]/(2A_i)^{1/2}$.[19]

Another heating mechanism that can contribute to the ion temperature is the friction between the ion species with different charge states. The ion temperature attributed to this mechanism can be estimated by integration of the energy contribution from the friction force R along the ion path

$$n_i V T_i \sim RL\Delta v. \quad (15)$$

Here, the friction force R is defined as $R\sim \nu_{ii} m_i n_i \Delta v$, where Δv is the velocity difference between ion species. If the friction is strong, $\lambda_{ii} \ll L$, $V\sim V_s$, and $\Delta v \sim V_s^2/(\nu_{ii}L)$; note that $\Delta v/V_s \sim \lambda_{ii}/L \ll 1$. We now readily obtain for the ion temperature:

$$T_i \sim m_i V_s^3/(\nu_{ii}L) \sim 0.03\ \mathrm{eV}. \quad (16)$$

The calculations performed above predict the ion temperature to be on the order of 0.05 eV, which is not consistent with the results of the experiments carried out in the SMIS 37 device demonstrating the effective temperature of several electron-volts.[17] However, plausible explanation of this strong heating can be given by means of ionization in the plasma flow as the ions travel from the center of the trap toward the extraction electrode. We now use Eqs. (1)–(3) to estimate the effective temperature of the ion flow. It should be noted that due to high plasma density in SMIS 37 the mean free path of a neutral atom with respect to electron impact ionization, i.e., $\lambda_i \sim \langle Z\rangle n_i K_i v_n \sim 0.04$ cm, is smaller than the plasma column radius. Here, $K_i=0.6\times 10^{-7}$ cm^3 s^{-1} is the ionization rate in nitrogen[20] and $v_n \sim \sqrt{T_r/m_i}$ is the neutral gas thermal velocity, where T_r is the room temperature. Therefore, one can expect a hollow radial density profile of the neutral gas density. The analysis of the radial profiles of the ion flow parameters is out of the scope of this paper, therefore for the purposes of this work, it is sufficient to consider all quantities as averaged over the plasma column cross section. Yet, we note that characteristic time for the thermal diffusion across the flow is comparable to the ion time of flight from the center to the exit of the magnetic trap, therefore the ion flow temperature can be on the same order across the flow. We assume the following

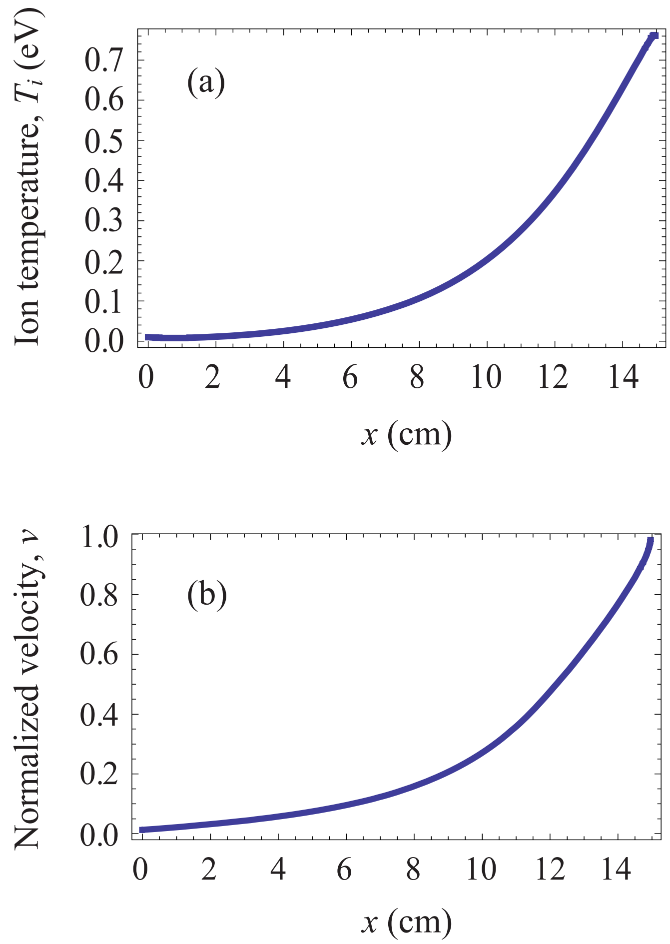

FIG. 3. (Color online) Numerical solution to the Eqs. (1)–(3) for the parameters characteristic of the SMIS 37 device. Spatial evolution of the ion flow parameters: (a) Flow temperature T_i; (b) normalized flow velocity v.

profile of the ion flow cross-section area: $S(x)=S_0B_0/B(x)$, where S_0 and B_0 are the plasma column radius and the on-axis magnetic field strength at the center of the trap, respectively. The on-axis magnetic field profile $B(x)$ used in the modeling is shown in Fig. 2(b). To describe ionization we adopt a simple model in which $J(x)$ is defined as $J(x)=\langle Z\rangle n(x) n_a K_i S(x)$, where $n(x)$ and n_a are the number densities of plasma ions and neutral atoms, respectively; and $K_i=0.6\times 10^{-7}$ cm^3 s^{-1} is the ionization rate in nitrogen. Finally, we assume that the neutral gas number density n_a is a constant along the ion flow, and we find n_a to match the condition $V=V_s$ at the minimum of the flow cross-section area; i.e., $S=S(x_m)$ (see Fig. 2). The solution of Eqs. (1)–(3) in the region $x\in[0;x_m]$ is shown in Fig. 3. For the initial conditions, we take $T_{i0}=10^{-2}$ eV, which is on the order of the value given by the collisional electron-ion heating, $V_0=\sqrt{\gamma T_{i0}/m_i}$, and $n_0=10^{13}$ cm^{-3}. Other parameters correspond to typical parameters of SMIS 37: $T_e=70$ eV, $Z_i=\langle Z\rangle=1.5$, $A_i=14$, $\gamma=5/3$. Matching condition, i.e., $V(x_m)=V_s$, gives $n_a=0.025n_0$, which is consistent with the parameters characteristic of SMIS 37. This value of the neutral gas density can be used to estimate the averaged effect of the ion-neutral charge-exchange collision on the ion flow dynamics. The corresponding mean free path is given by

$\lambda_{chxg}^{i\to n} \sim 1/(n_a\sigma_{chxg})=607$ cm and is much greater than the trap length. Here, $\sigma_{chxg}\sim 65.8\times 10^{-16}$ cm^2 is the value of the charge-exchange cross section in nitrogen.[21] Note that the characteristic length of neutral gas ionization by electron impact, i.e., $\lambda_i \sim 0.04$ cm, is much smaller than the mean free path of a neutral atom with respect to charge-exchange collisions with ions, $\lambda_{chxg}^{n\to i}\sim v_n/(v_i n_i \sigma_{chxg})\sim 0.24$ cm, where $v_i \sim \sqrt{\langle Z\rangle T_e/m_i}$ is the ion axial velocity. Therefore, cold neutral atoms are promoted to the ionized state by electron impact ionization, and the neutral gas heating due to charge-exchange processes is negligible. Figure 3(a) shows that as the flow leaves the magnetic plug at $x=x_m$, the ion temperature becomes about 1 eV, which is on the order of the temperature measured in the experiments.

It should be noted that as the ion flow temperature reaches a few electron-volts, the ion mean free path becomes comparable to the trap length ($\lambda_{ii}\sim L$) and the single ion fluid description is no longer valid; that is, different ion species cannot be represented by a single ion fluid with an average charge state $\langle Z\rangle$. Note that ion heating due to the friction between different ion species is significantly increased when $\lambda_{ii}\sim L$. In this case, $\Delta v \sim V_s$, and the ion temperature in the spreading region ($x\in[x_m;x_m+d]$) can be estimated by

$$T_i \sim \nu_{ii} m_i V_s d \sim 23 \text{ eV}. \tag{17}$$

Therefore, this heating mechanism can lead to a further increase of the ion temperature in the plasma spreading region.

IV. IONIZATION HEATING IN AN ECR ION SOURCE WITH THE CLASSICAL REGIME OF PLASMA CONFINEMENT

The considered in this paper mechanism of ion heating due to ionization in a plasma flow is also present in the ECR sources with the classical regime of confinement (the electron-ion collision frequency is low, and the electron loss cone is almost empty). However, in this section we demonstrate that ion heating attributed to this mechanism is much less compared to that in gas-dynamic ECR ion sources. Figure 4 shows the velocity phase-space at the center of the magnetic trap for the case of the classical regime of confinement. Most of the electrons are reflected by the magnetic field variations and do not reach the magnetic plug. Only a small fraction of electrons that is confined in the trap by means of the ambipolar potential barrier φ_A reaches the magnetic plug. Note that the electron loss cone is almost empty ($\varphi_A \ll T_e/e$). Detailed information regarding the ambipolar potential variations in ECR ion sources, as well as the characteristic values of the plasma density and temperature corresponding to the classical and the quasi-gas-dynamic regimes of plasma confinement can be found in Ref. 11. Typically, ions are cold in the classical ECR ion sources ($\lambda_{ii}\ll L$), and the fluid equations can be applied to describe ion acceleration. However, for the case of the classical regime of confinement ions are accelerated by the ambipolar potential only to the velocity of $V_{cl}\sim\sqrt{eZ_i\varphi_A/m_i}$, and therefore the characteristic ion temperature attributed to the ion-

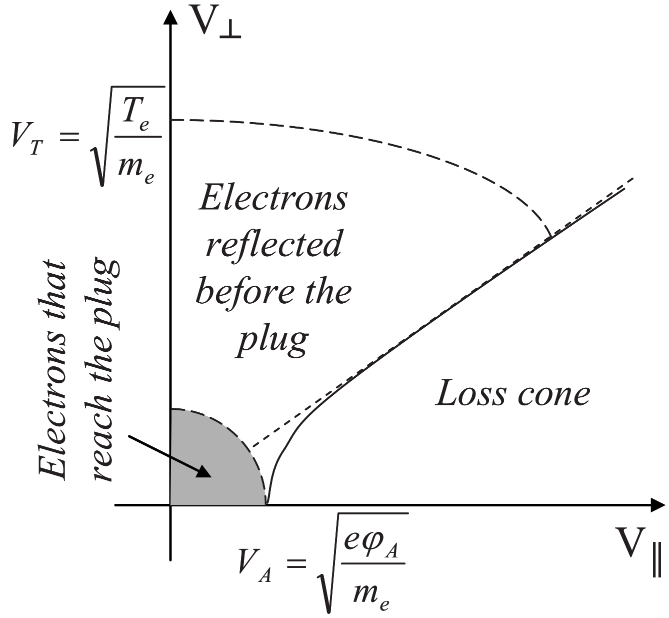

FIG. 4. The velocity phase-space in the center of the magnetic trap for the case of the classical regime of plasma confinement $e\varphi_A \ll T_e$.

ization heating is now given by $T_{cl}\sim 0.06[(\gamma-1)/\gamma]Z_i e\varphi_A$, which is much less compared to the case of the quasi-gas-dynamic confinement.

It should be noted that the ambipolar potential barrier φ_A can be estimated if the ion species can be described by means of fluid equations, provided by $\lambda_{ii}\ll L$. Indeed, the electron density in the plug (n_a) is given by

$$n_a \sim n_{e0} V_A^3/V_T^3. \tag{18}$$

Here, n_{e0} is the electron density in the center of the trap, $V_T=\sqrt{T_e/m_e}$ is the electron thermal velocity, $V_A=\sqrt{e\varphi_A/m_e}$ is the characteristic electron velocity defined by the potential barrier, and m_e is the electron mass. Assuming quasineutrality, the ion flux Γ_i leaving the trap is given by

$$\Gamma_i = n_a V_{cl} S_p / Z_i, \tag{19}$$

where S_p is the flow cross-section area at the magnetic plug. At the same time, electrons are scattered to the loss cone and leave the trap at the rate of

$$\Gamma_e \sim n_{e0} L S \nu_{ei}, \tag{20}$$

where S is the characteristic cross-section area of the plasma flow (in the case of large mirror ratio $S\gg S_P$). Making use of the global charge balance equation, i.e., $\Gamma_e = Z_i\Gamma_i$, we readily obtain

$$\frac{V_A^4}{V_T^4} = \frac{S}{S_P}\frac{L}{\sqrt{Z_i T_e/m_i}}\nu_{ei}. \tag{21}$$

It readily follows from Eq. (21) that the condition for the classical regime of confinement, which corresponds to the almost empty electron loss cone (or, equivalently, $\varphi_A \ll T_e/e$) is given by

$$\nu_{ei} \ll \frac{S_p}{S} \frac{\sqrt{Z_i T_e/m_i}}{L}. \quad (22)$$

Note that for the case of $S \sim S_P$ and $T_e \gg T_i$, estimate (22) reduces to $\nu_{ei} \ll V_s/L$, which is opposite to the condition for the quasi-gas-dynamic regime of confinement: $\nu_{ei} \gg V_s/L$.

V. CONCLUSION

A mechanism of ion heating attributed to ionization in a plasma flow with hot electrons and initially cold ions has been studied by means of fluid equations for the ion flow density, velocity, and temperature. It has been shown that the initially cold ion flow can reach a temperature on the order of several hundredths of the electron temperature, as the ions are accelerated to the ion-acoustic speed, provided there is significant ionization in the acceleration region. For the case of constant flow cross-section area the final ion temperature is given by $T_i \approx 0.07(\gamma - 1)/\gamma Z_i T_e$, where Z_i is the ion charge and γ is the adiabatic gamma factor. Analyzing results of the theoretical studies for parameters characteristic of the gas-dynamic electron cyclotron resonance (ECR) ion source SMIS 37 yields much higher effective ion temperature than can be attributed to the electron-ion collisional energy transfer, typically considered for classical ECR ion sources. This theoretical result is found to be in agreement with findings of recent experiments carried out in SMIS 37.

Ion heating due to ionization is also present in ECR ion sources with the classical regime of plasma confinement. It is, however, much less compared to that in gas-dynamic ECR ion sources, and can provide ion heating only to the temperatures much less than the electron temperature.

ACKNOWLEDGMENTS

The authors are grateful to L. A. Dorf for fruitful discussions.

This research was supported by ISTC Grant No. 2753 and RFBR Grant No. 06-02-22002.

[1] L. Tonks and I. Langmuir, Phys. Rev. **34**, 876 (1929).
[2] K.-B. Persson, Phys. Fluids **5**, 1625 (1962).
[3] S. A. Self and H. N. Ewald, Phys. Fluids **9**, 2486 (1966).
[4] G. A. Emmert, R. M. Wieland, A. T. Mense, and J. N. Davidson, Phys. Fluids **23**, 803 (1980).
[5] K.-U. Riemann, Phys. Fluids **24**, 2163 (1981).
[6] J. T. Scheuer and G. A. Emmert, Phys. Fluids **31**, 1748 (1988).
[7] J. T. Scheuer and G. A. Emmert, Phys. Fluids B **2**, 445 (1990).
[8] D. Leitner and C. Lyneis, "ECR Ion Sources," in *The Physics and Technology of Ion Sources*, edited by I. G. Brown (John Wiley & Sons, New York, 2004), Chap. 11.
[9] V. V. Mirnov and D. D. Ryutov, Pis'ma Zh. Tekh. Fiz. **5**, 678 (1979).
[10] V. Semenov, A. Smirnov, and A. Turlapov, Fusion Technol. **35**, 398 (1999).
[11] V. Semenov, V. Skalyga, A. Smirnov, and V. Zorin, Rev. Sci. Instrum. **73**, 635 (2002).
[12] S. V. Golubev, S. V. Razin, V. E. Semenov, A. N. Smirnov, A. V. Vodopyanov, and V. G. Zorin, Rev. Sci. Instrum. **71**, 669 (2000).
[13] A. Sidorov, A. Bokhanov, I. Izotov, S. Razin, V. Skalyga, V. Zorin, A. Balabaev, S. Kondrashev, R. Geller, T. Lamy, P. Sortais, T. Thuillier, and P. Spädtke, Rev. Sci. Instrum. **77**, 03A341 (2006).
[14] S. Golubev, I. Izotov, S. Razin, V. Skalyga, A. Vodopyanov, and V. Zorin, Fusion Sci. Technol. **47**, 345 (2005).
[15] V. Zorin, S. Golubev, S. Razin, A. Sidorov, V. Skalyga, and A. Vodopyanov, Rev. Sci. Instrum. **75**, 1675 (2004).
[16] V. Skalyga, V. Zorin, I. Izotov, S. Razin, A. Sidorov, and A. Bokhanov, Plasma Sources Sci. Technol. **15**, 727 (2006).
[17] A. Sidorov, M. Dorf, V. Zorin, A. Bokhanov, I. Izotov, S. Razin, V. Skalyga, P. Spädtke, J. Roßbach, and A. Balabaev, Rev. Sci. Instrum. **79**, 02A317 (2008).
[18] G. Melin, A. G. Drentje, A. Girard, and D. Hitz, J. Appl. Phys. **86**, 4772 (1999).
[19] J. D. Huba, *Revised NRL Plasma Formulary* (Naval Research Laboratory, Washington, D.C., 2000).
[20] G. S. Voronov, At. Data Nucl. Data Tables **65**, 1 (1997).
[21] B. J. Nichols and F. C. Witteborn, NASA Technical Note No. D-3265 (1966).